Magnetic-Flux Pumping in High-Performance, Stationary Plasmas with Tearing Modes

C. C. Petty, M. E. Austin,* C. T. Holcomb,† R. J. Jayakumar,† R. J. La Haye, T. C. Luce, M. A. Makowski,† P. A. Politzer, and M. R. Wade

General Atomics, P.O. Box 85608, San Diego, California 92186, USA

(Received 17 January 2008; published 30 January 2009)

Analysis of the change in the magnetic field pitch angles during edge localized mode events in high performance, stationary plasmas on the DIII-D tokamak shows rapid (<1 ms) broadening of the current density profile, but only when a $m/n = 3/2$ tearing mode is present. This observation of poloidal magnetic-flux pumping explains an important feature of this scenario, which is the anomalous broadening of the current density profile that beneficially maintains the safety factor above unity and forestalls the sawtooth instability.

DOI: 10.1103/PhysRevLett.102.045005 PACS numbers: 52.55.Fa, 52.35.Vd, 52.70.Ds

The anomalous transport of magnetic flux is a process widespread in both laboratory and astrophysical plasmas. The mechanisms include magnetic reconnection [1], self-generation of magnetic fields (dynamo effect) [2], and convective pumping of magnetic flux [3]. This suite of physics can be referred to under the general heading of ''magnetic-flux pumping.'' In this Letter, a sensitive and localized diagnostic of the internal magnetic structure of tokamaks is used to determine the role of magnetic-flux pumping in high performance, stationary plasmas with tearing modes that are an attractive operating scenario for burning plasma experiments. The performance characteristics of these plasmas are intermediate between the standard, high current, high confinement (H-mode) scenario [4] and the steady-state advanced tokamak scenario [5]; hence, this is referred to as the ''hybrid'' scenario. An important feature of the hybrid scenario is that the plasma current profile is broader than expected for resistive diffusion, which stabilizes the sawtooth instability [6,7] by elevating the safety factor (q) everywhere above unity. (The safety factor is defined as the spatial rate of change of toroidal magnetic flux with poloidal magnetic flux.) This eliminates a trigger for the deleterious $m/n = 2/1$ neoclassical tearing mode (NTM) and allows hybrid scenario plasmas to operate at high β. Here β is the ratio of the plasma kinetic pressure to the magnetic field pressure, and NTMs are magnetic islands with poloidal mode number m and toroidal mode number n that grow owing to a helical deficit in the bootstrap current that is resonant with the spatial structure of the local magnetic field at $q = m/n$ [8].

Several realizations of the hybrid scenario have been reported from the ASDEX-U [9], JET [10], and JT-60U [11] tokamaks, as well as from the DIII-D [12,13] tokamak which is the subject of this Letter. A key previous experiment in hybrid plasmas on DIII-D demonstrated that when the $m/n = 3/2$ NTM does not form or is suppressed by electron cyclotron current drive, the central safety factor decreases below unity and the discharge begins to sawtooth [14]. In addition, anomalous broadening of the plasma current profile is not evident when the minimum in the safety factor ($q_{\min}$) is greater than ≈ 1.05. In this Letter, we show for the first time that coupling between two MHD instabilities, the continuous $m/n = 3/2$ NTM and the periodic edge localized mode (ELM), results in a cyclic broadening of the current density profile in hybrid discharges due to magnetic-flux pumping. Direct evidence for this comes from motional Stark effect (MSE) polarimetry [15,16], which measures the profile of the magnetic field pitch angles near the median plane of the plasma with a radial resolution of 0.015–0.05 m.

The cyclic modification of the $m/n = 3/2$ island size and plasma current density during ELMs is shown in Fig. 1 for a hybrid plasma on DIII-D with $q_{95} = 4.35$ (referring to the 95% normalized poloidal flux surface) and $\beta = 2.8\%$. Typical parameters for DIII-D are major radius $R = 1.7$ m, minor radius $a = 0.6$ m, toroidal magnetic field $B_T = 1.7$ T, and plasma current $I_p = 1.2$ MA. ELMs are short, repetitive perturbations in the plasma edge that are generally observed in H-mode discharges; the limiting instability has been successfully modeled as a peeling-ballooning mode of intermediate toroidal mode number ($3 < n < 30$) [17,18]. This perturbation is easily identified by the spike in the Balmer-alpha light from the plasma edge. Figure 1 shows that the $m/n = 3/2$ island width is modulated by the ELMs, with the width decreasing by up to 40% in <1 ms, then typically recovering in 5–10 ms [19]. The coupling between the ELM and NTM is confirmed by a steepening of the electron temperature (T_e) gradient at the island location, as seen in Fig. 2. This figure plots the change in the electron temperature (ΔT_e) using 5 ms averaging preceding and following the ELM event as a function of the normalized toroidal flux coordinate (ρ). The ELM causes a localized increase in ∇T_e centered on the $q = 3/2$ surface; the apparent decrease in T_e of 20–40 eV is a result of the vertical (not radial) shift of the plasma by ≤ 0.03 m at the ELM time from equilibrium reconstructions. Figure 2 also shows the measured modulation of the electron cyclotron emission (ECE) signals ($\tilde{T}_e$) at the island

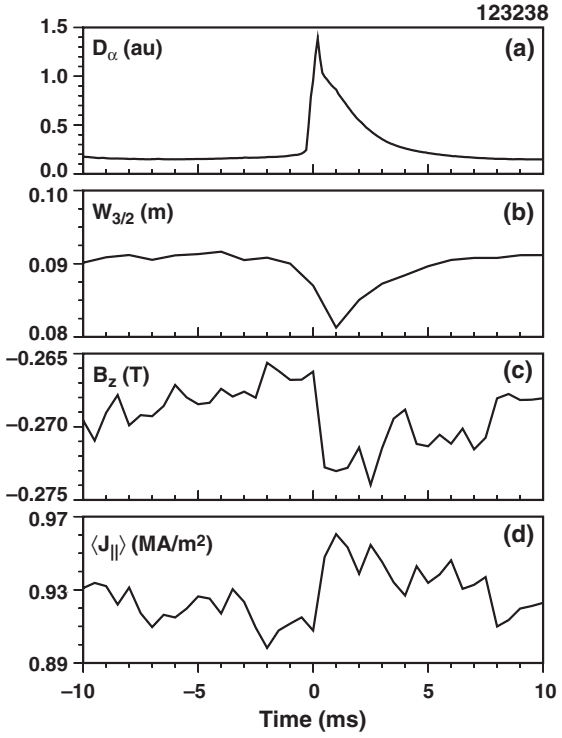

FIG. 1. Time histories relative to ELM event ($t = 0$) of (a) Balmer-alpha light from divertor, (b) width of $m/n = 3/2$ island, (c) vertical magnetic field strength inside island measured by MSE, and (d) flux-surface-average parallel current density inside island. The signals are averaged over 112 ELMs.

rotation frequency ($\approx$20 kHz), which is proportional to the radial displacement of the $q = 3/2$ surface. The measured phase of the ECE fluctuation is observed to shift by $\approx$180° around $\rho = 0.41$, which is identified as the island O-point location. The $\tilde{T}_e$ profile is complicated by the presence of $(m \pm 1)/n$ sidebands to the $m/n = 3/2$ mode that are resonant with the $q = 1$ and $q = 2$ surfaces.

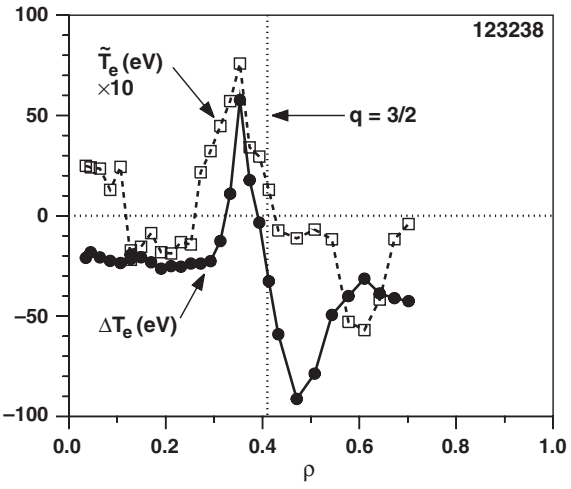

FIG. 2. Radial profiles of the change in electron temperature during an ELM (ΔT_e), averaged over 112 ELMs, and the amplitude of the electron temperature fluctuation at the rotation frequency of the $m/n = 3/2$ NTM ($\tilde{T}_e$). The sign of $\tilde{T}_e$ indicates whether the fluctuations are in phase or out of phase with a magnetic probe.

Figure 1 shows that during the ELM event, the vertical magnetic field strength (B_z), measured by midplane MSE polarimetry, increases in magnitude (becomes more negative) at the $m/n = 3/2$ island location. The change in B_z is rapid, occurring in $<$1 ms, which is near the maximum time resolution available with the standard MSE setup on DIII-D (2 kHz digitization rate). Figure 1 also shows that the (axisymmetric) flux-surface-average parallel current density ($\langle J_\parallel \rangle$), determined directly from the MSE signals without equilibrium reconstruction using Ampère's law [20], also increases rapidly ($<$1 ms) at the $m/n = 3/2$ island location during the ELM. Between ELMs, B_z and $\langle J_\parallel \rangle$ relax to their pre-ELM values as the poloidal magnetic flux diffuses on the resistive time scale (tens of ms), which is given by $\tau_\eta \approx \mu_0 \Delta^2/\eta$, where Δ is a characteristic scale length in the plasma and η is the plasma electrical resistivity. No change in the B_z or $\langle J_\parallel \rangle$ profiles near the $q = 3/2$ surface is expected during ELMs as a result of the change in T_e profile shown in Fig. 2 (except for a possible change in the bootstrap current).

The rapid changes in the MSE signals during an ELM are due to a broadening of the current density profile and an increase in the central safety factor, as shown in Fig. 3. For this hybrid plasma with $q_{95} = 4.4$ and $\beta = 3.1\%$, the profile changes are determined by subtracting the mean value during the 5 ms before the ELM from the mean value during the 5 ms after the ELM. Figure 3 shows that the

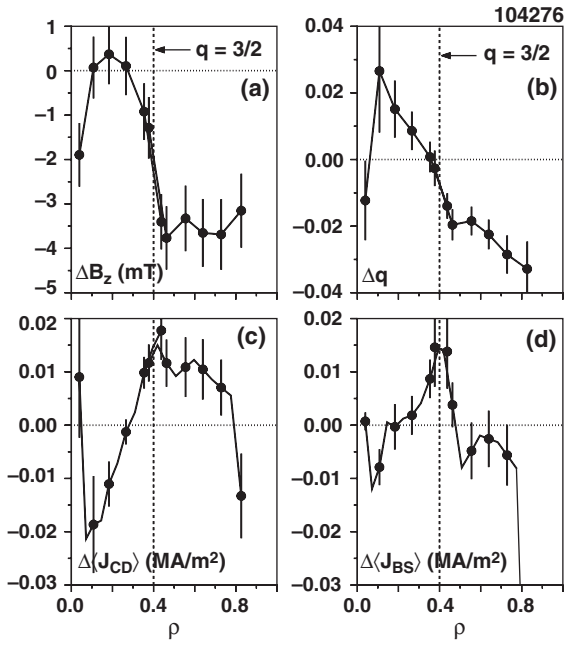

FIG. 3. Radial profiles of the change during an ELM of (a) vertical magnetic field strength measured by MSE, (b) safety factor, (c) externally driven current density, and (d) bootstrap current density. The MSE signals are averaged over 39 ELMs.

measured B_z profile changes relatively little for radii smaller than the $m/n = 3/2$ NTM location (which is at $\rho = 0.4$), but for larger radii the magnitude of B_z increases (becomes more negative) after the ELM. This change in the B_z profile cannot be explained by movement of the plasma flux surfaces; the major radius of the plasma axis shifts by ≤ 0.001 m during the ELM, and the MSE midplane measurements are not sensitive to small vertical shifts of the plasma. The changes in the safety factor and current density profiles can be determined from a direct analysis of the MSE signals without equilibrium reconstruction (although a few basic geometric parameters need to be known) [20]. As seen in Fig. 3, the q value decreases outside of the $q = 3/2$ surface during the ELM, whereas q increases by ≈ 0.02 near the axis [right on axis the slightly reversed q profile flattens, which explains the negative $\Delta q(0)$]. The broadening of the $\langle J_\parallel \rangle$ profile during the ELM is examined in Fig. 3 by plotting separately the bootstrap current component ($\langle J_{\mathrm{BS}} \rangle$) and the external current drive component ($\langle J_{\mathrm{CD}} \rangle = \langle J_\parallel \rangle - \langle J_{\mathrm{BS}} \rangle$). The direct analysis of the MSE signals shows that a small amount of externally driven current (~ 2 kA) is displaced from inside to outside the $q = 3/2$ surface during the ELM. The bootstrap current density is observed to increase at the $m/n = 3/2$ NTM location following the ELM, which is consistent with the measured increase in the temperature gradient (Fig. 2).

Although the change in the safety factor profile during an ELM is not large, the ELM frequency is high enough to keep the q profile elevated above unity and forestall the occurrence of sawteeth. Simulations of the poloidal magnetic-flux evolution for the hybrid plasma in Fig. 3 show that the time scale for q_{min} to evolve by 0.02 is $\approx$ 55 ms, which is a little longer than the measured ELM period of ≈ 40 ms. Therefore, the ELM cycle is rapid enough compared to the magnetic diffusion time scale to maintain a current density profile constantly broader than the fully relaxed state. Another issue is the fast change (<1 ms) in the current density seen in Fig. 1, which occurs too rapidly to be a diffusive process and connotes an Alfvén time scale. While we offer no conjecture as to how the coupling between the ELM and $m/n = 3/2$ NTM can broaden the current density profile, we note that the rapid redistribution of current to larger radii during ELMs resembles the sawtooth instability whereby current in the core of the plasma is periodically redistributed during the sawtooth crash [21,22]. The sawtooth oscillation is unstable to the $m/n = 1/1$ internal kink and the current redistribution occurs around the $q = 1$ surface, whereas hybrid plasmas have an unstable $m/n = 3/2$ NTM and the current redistribution occurs around the $q = 3/2$ surface. The net effect of these cyclic mechanisms is to transport (or pump) poloidal magnetic flux across magnetic field lines, resulting in the poloidal magnetic-flux profile maintaining a constant shape against diffusion (when averaged over many cycles), which is a necessary condition for the current density profile to be stationary on long time scales. A notable difference between these phenomena is that, for the sawtooth instability, the $m/n = 1$ island grows during the current redistribution, whereas here the $m/n = 3/2$ island shrinks.

The cyclic broadening of the current density profile during ELMs is only observed when a $m/n = 3/2$ NTM is present in the hybrid plasma. Figure 4 shows a comparison of the poloidal magnetic-flux pumping between a hybrid plasma ($q_{95} = 4.35$ and $\beta = 2.95\%$) with a $m/n = 3/2$ NTM and a similar plasma ($q_{95} = 4.7$ and $\beta = 2.95\%$) with a $m/n = 5/3$ NTM. The sawtooth instability is observed in the $m/n = 5/3$ NTM discharge but not in the $m/n = 3/2$ discharge, which is consistent with measurements of $q_{\mathrm{min}} = 0.99$ for the former case and $q_{\mathrm{min}} = 1.02$ for the latter case. The measured change in the MSE signals for the $m/n = 5/3$ NTM plasma in Fig. 4 shows no discernible broadening of the current density profile during the ELM event. A similar negative result is obtained for discharges with a $m/n = 4/3$ NTM. An explanation for the different sawtooth suppression behavior between the $m/n = 3/2$ and $m/n = 5/3$ NTMs may be that the former possesses a $(m-1)/n$ sideband that is resonant with $q = 1$ while the latter does not (note that the amplitude of the $m/n = 2/2$ sideband increases rapidly as q_{min} approaches 1) [23]. Although the $m/n = 4/3$ NTM also has a sideband resonant with $q = 1$, measurements of the electron temperature profile find no evidence that ELMs couple to the $q = 4/3$ surface. Rather, the localized increase in ∇T_e following an ELM is either centered on the $q = 5/3$ island (similar to Fig. 2 but at larger radii) or is not present at all. Additionally, it is possible that the $q = 2$ surface, resonant with a $(m+1)/n$ sideband of the $m/n = 3/2$ (or 5/3) NTM, may be playing a role in the linkage between the edge and core plasmas during ELMs, although there is no direct experimental confirmation of this.

Finally, the strength of the poloidal magnetic-flux pumping in hybrid plasmas with a $m/n = 3/2$ NTM appears to increase with β. This is shown in Fig. 5, where the change

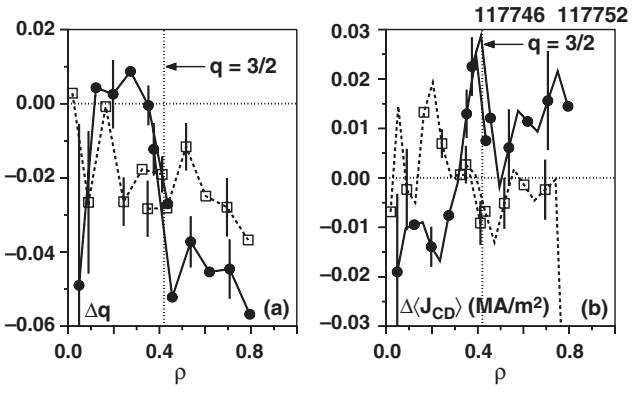

FIG. 4. Radial profiles of the change during an ELM of (a) safety factor and (b) externally driven current density. Solid lines are for a hybrid plasma with a $m/n = 3/2$ NTM while dashed lines are for a similar plasma with a $m/n = 5/3$ NTM. The data are averaged over ≈ 20 ELMs.

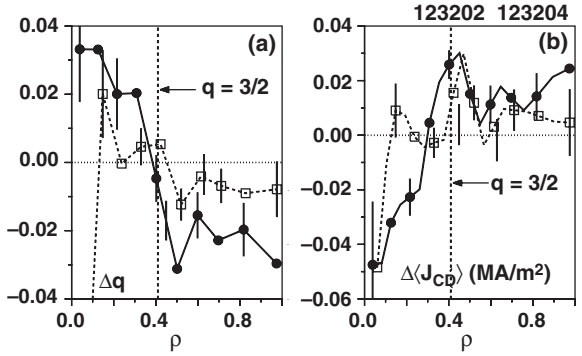

FIG. 5. Radial profiles of the change during an ELM of (a) safety factor and (b) externally driven current density for hybrid plasmas with a $m/n = 3/2$ NTM. Solid lines are for a discharge with $\beta = 2.95\%$ and $q_{95} = 4.65$ while dashed lines are for a discharge with $\beta = 2.2\%$ and $q_{95} = 4.4$. The data are averaged over ≈ 15 ELMs.

in the q and $\langle J_{CD}\rangle$ profiles are compared between hybrid discharges with $\beta = 2.25\%$ and $\beta = 2.95\%$. The lower β plasma has an ≈ 0.05 lower value of $q_{\min}$ than the higher β plasma, consistent with only the lower β case having sawteeth. Figure 5 shows that, for the lower β discharge, the changes in the q and $\langle J_{CD}\rangle$ profiles during ELMs are smaller compared to the higher β discharge. This behavior may be due to the increase in the radial depth of the ELM with higher β which, combined with the relatively low-n peeling-ballooning modes found in low density plasmas, increases the linkage between edge and core MHD [18].

Previous publications have suggested other possible roles for the $m/n = 3/2$ NTM in maintaining $q_{\min}$ above unity in hybrid plasmas. For example, it has been theorized that counter current drive near the axis may be induced by the $m/n = 2/2$ component of the NTM that develops when $q_{\min}$ approaches 1 [23]. Another suggestion is that the NTM may cause radial transport of fast ions (independent of ELMs), which can broaden the neutral beam current drive profile [23]. While these other mechanisms are not ruled out by the MSE measurements of poloidal magnetic-flux pumping during ELMs discussed in this Letter, our present mechanism appears to be sufficient to explain why the safety factor remains above unity in hybrid plasmas.

In conclusion, rapid broadening of the current density profile during the ELM modification of the $m/n = 3/2$ NTM in hybrid plasmas has been measured on the DIII-D tokamak using direct analysis of the MSE signals without equilibrium reconstruction. The measured safety factor profile increases inside of the $q = 3/2$ surface and decreases outside of it during the ELM. The resulting poloidal magnetic-flux pumping is large enough, and the ELM frequency is high enough, to maintain the safety factor profile slightly above unity and forestall the occurrence of sawteeth (for $q_{95} > 4$). The coupling between the ELM and the NTM is confirmed by the measured increase in the electron temperature gradient near the resonance q surface following the ELM event. A discernible broadening of the current density profile during ELMs occurs only in the presence of the $m/n = 3/2$ NTM, and appears to increase with β. The rapid (<1 ms) broadening of the current density profile during ELMs connotes an Alfvén time scale and appears to be similar to the redistribution of current during a sawtooth crash (although around a different resonant q surface). The significance of the $m/n = 3/2$ mode may be that this NTM possesses a sideband that is resonant with $q = 1$, whereas the $m/n = 5/3$ NTM, which also shows strong coupling to ELMs, does not. Future experiments will attempt to verify the role of ELMs in maintaining the broad current density profile in hybrid plasmas by changing the neutral beam injection angle or applying resonant magnetic perturbations to suppress the ELMs.

This work was supported by the U.S. Department of Energy under DE-FC02-04ER54698, DE-FG03-97ER54415, and W-7405-ENG-48.

*Also at University of Texas at Austin, Austin, TX, USA.
†Also at Lawrence Livermore National Laboratory, Livermore, CA, USA.

[1] Y. Kikuchi *et al.*, Phys. Rev. Lett. **97**, 085003 (2006).
[2] W. X. Ding *et al.*, Phys. Rev. Lett. **93**, 045002 (2004).
[3] J. H. Thomas *et al.*, Nature (London) **420**, 390 (2002).
[4] R. Aymar, P. Barabaschi, and Y. Shimomura, Plasma Phys. Controlled Fusion **44**, 519 (2002).
[5] T. S. Taylor *et al.*, Plasma Phys. Controlled Fusion **39**, B47 (1997).
[6] S. von Goeler, W. Stodiek, and N. Sauthoff, Phys. Rev. Lett. **33**, 1201 (1974).
[7] B. B. Kadomtsev, Sov. J. Plasma Phys. **1**, 389 (1975).
[8] Z. Chang *et al.*, Phys. Rev. Lett. **74**, 4663 (1995).
[9] A. C. C. Sips *et al.*, Plasma Phys. Controlled Fusion **44**, B69 (2002).
[10] E. Joffrin *et al.*, Plasma Phys. Controlled Fusion **45**, A367 (2003).
[11] A. Isayama *et al.*, Nucl. Fusion **43**, 1272 (2003).
[12] T. C. Luce *et al.*, Nucl. Fusion **41**, 1585 (2001).
[13] M. R. Wade *et al.*, Phys. Plasmas **8**, 2208 (2001).
[14] M. R. Wade *et al.*, Nucl. Fusion **45**, 407 (2005).
[15] F. M. Levinton *et al.*, Phys. Rev. Lett. **75**, 4417 (1995).
[16] B. W. Rice *et al.*, Phys. Rev. Lett. **79**, 2694 (1997).
[17] J. W. Connor *et al.*, Phys. Plasmas **5**, 2687 (1998).
[18] P. B. Snyder *et al.*, Phys. Plasmas **9**, 2037 (2002).
[19] T. C. Luce *et al.*, Phys. Plasmas **11**, 2627 (2004).
[20] C. C. Petty, P. A. Politzer, and Y. R. Lin-Liu, Plasma Phys. Controlled Fusion **47**, 1077 (2005).
[21] H. Soltwisch, Rev. Sci. Instrum. **59**, 1599 (1988).
[22] D. Wróblewski and R. T. Snider, Phys. Rev. Lett. **71**, 859 (1993).
[23] P. A. Politzer *et al.*, in *Proceedings of the 32nd European Conference on Plasma Physics, Tarragona, 2005* (EPS, Geneva, 2005), Vol. 29C, p. O-1.001.